



OPEN

Long-term variation of ^{90}Sr and ^{137}Cs in environmental and food samples around Qinshan nuclear power plant, China

Yiyao Cao^{1,4}, Zhixin Zhao^{2,4}, Peng Wang¹, Shunfei Yu¹, Zhongjun Lai¹, Meibian Zhang³, Xiangjing Gao¹, Yaoxian Zhao¹, Zhiqiang Xuan¹, Hong Ren¹, Dongxia Zhang¹ & Xiaoming Lou¹✉

Environmental radioactivity monitoring in the surroundings of nuclear facilities is important to provide baseline data for effective detection in case of any radioactive release in the region. In this work, we report for the first time the long-term monitoring data of ^{137}Cs and ^{90}Sr in environmental and food samples around Qinshan nuclear power plant in 2012–2019. The distribution levels, temporal variations and source terms of ^{137}Cs and ^{90}Sr in the investigated samples were discussed. The annual effective dose (AED) for the local population from the ingestion of foods was also evaluated. Peak values of ^{90}Sr and ^{137}Cs concentrations and $^{137}\text{Cs}/^{90}\text{Sr}$ activity ratio were observed in total atmospheric deposition in 2016 and some water and food samples in the following years. This seems to be associated to an additional radioactive input, mostly likely from the operational release of a local facility. This demonstrates that ^{90}Sr and ^{137}Cs , especially the $^{137}\text{Cs}/^{90}\text{Sr}$ activity ratio, are sensitive indicators for detecting potential radioactive releases. Nevertheless, overall ^{90}Sr and ^{137}Cs activity concentrations measured during 2012–2019 in this work were at the background levels with average AED far below the internationally permissible limit and recommendation.

Over the past decades, the proportion of energy sourced from nuclear power has increased rapidly worldwide. China has vigorously developed nuclear power in recent years¹. Systematic monitoring of important anthropogenic radionuclides is crucial for revealing sources and transport pathways in case of severe accidental or deliberate releases of radioactive pollutants. Among the radionuclides released from the operation of nuclear facilities and nuclear accidents, the two high-yield fission products ^{90}Sr ($t_{1/2} = 28.79$ y) and ^{137}Cs ($t_{1/2} = 30.17$ y) are recognized as the most important from the radiological perspective². Due to their relatively long half-lives, ^{90}Sr and ^{137}Cs can be preserved in terrestrial and marine systems for a long time once entering the environment. Under natural environmental conditions, ^{137}Cs and ^{90}Sr mainly enter the human body through the food chain and respiration. Both ^{90}Sr and ^{137}Cs have long biological half-lives in the human body^{3–8}, therefore it is important to continuously monitor ^{90}Sr and ^{137}Cs in environmental and food samples, especially those from the surroundings of nuclear facilities, to ensure the radiological safety of individuals and the environment. In contrast to ^{137}Cs , long-term monitoring data for ^{90}Sr activity in environmental and food samples worldwide are sparse. This fact is mainly attributed to the long and tedious sample preparation and measurement procedures for ^{90}Sr .

The Qinshan nuclear power plant (QNPP) is the first nuclear power plant in China and officially commenced commercial operation in December 1991. The QNPP is a multi-unit nuclear power plant, and consists of three phases NPPs operating two heavy water reactors (HWRs) and seven pressurized water reactors (PWRs) with a total installed capacity of ca. 6.5 GW. Artificial radionuclides such as ^3H and ^{14}C in the vicinity of QNPP have been investigated to a very limited extent during the past decades^{9,10}. Studies on primary fission products in environmental and foods samples, especially long-term systematic studies have not been reported so far. In this work, we report for the first time a long-term observation of ^{137}Cs and ^{90}Sr in environmental and food samples collected around QNPP during 2012–2019. The distribution levels, temporal variations and source terms of

¹Department of Occupational Health and Radiation Protection, Zhejiang Provincial Center for Disease Control and Prevention, Hangzhou 310051, Zhejiang, China. ²Hangzhou Hospital for the Prevention and Treatment of Occupational Disease, Hangzhou 310051, Zhejiang, China. ³National Institute of Occupational Health and Poison Control, Chinese Center for Disease Control and Prevention, Beijing 100050, China. ⁴These authors contributed equally: Yiyao Cao and Zhixin Zhao. ✉email: 540040349@qq.com

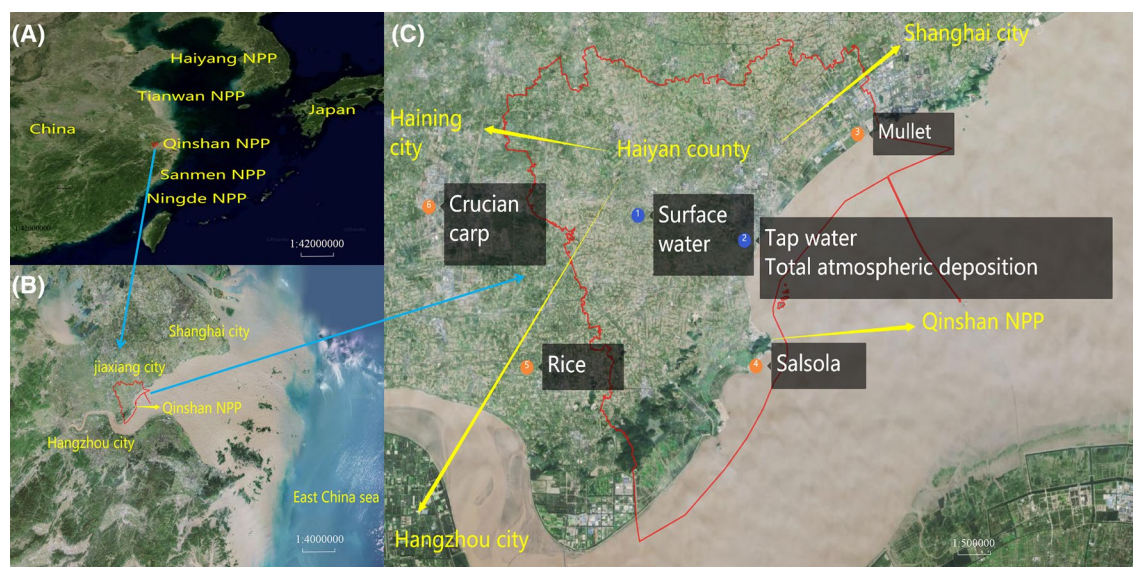


Figure 1. Map showing the geographical location of QNPP (A, scale: 1:42,000,000) and (B, scale: 1:4,000,000), and sampling sites in the surroundings of QNPP marked with filled circles and numbers (C, scale: 1:500,000). The map was produced using software MapInfo Professional using data from <https://bajiu.cn/ditu/>.

Sample category	Type or species	Location (coordinates)	Distance from QNPP (km)	Sampling frequency and time	Sample size	No. of subsamples
Fallout	Total atmospheric deposition	30° 31' 4" (N) 120° 55' 40" (E)	9.8	Quarterly End of every month	10 L	3
Water	Surface water	30° 32' 56" (N) 120° 49' 48" (E)	17.2	Twice per year May, October	50 L	3
	Tap water	30° 31' 4" (N) 120° 55' 40" (E)	9.8	Twice per year May, October	50 L	3
Food	Mullet	30° 33' 57" (N) 120° 1' 9" (E)	15.0	Annually May	10 kg	3
	Rice	30° 24' 20" (N) 120° 46' 52" (E)	18.8	Annually November	20 kg	3
	Salsola	30° 25' 41" (N) 120° 57' 22" (E)	1.8	Annually June	10 kg	3
	Crucian carp	30° 32' 19" (N) 120° 42' 49" (E)	26.9	Annually August	10 kg	3

Table 1. Samples collected from QNPP in this work during 2012–2019.

^{137}Cs and ^{90}Sr in the study region were investigated. The annual effective dose was estimated for the local public based on our measurement data.

Materials and methods

The study region and sample collection. The QNPP is located in Haiyan County, Jiaxing City, Zhejiang Province in China, close to Hangzhou Bay in the East China Sea, 130 km away from Shanghai, and 93 km away from Hangzhou (the capital of Zhejiang Province). All samples were collected within 30 km of QNPP during the period of 2012–2019 (Fig. 1), and the detailed sampling information is listed in Table 1.

Total (dry and wet) atmospheric deposition samples were monitored quarterly at a location 9.8 km away from QNPP. A total deposition collector (ZJC-VI deposition automatic collector, Zhejiang Hengda technology co.) with a surface area of 0.25 m² was placed on the open space of a building roof at Center for Disease Control and Prevention of Haiyan for sample collection. The sample was collected at the end of each month and bulked quarterly for radioactivity measurement.

Surface waters were collected in Qianmudang reservoir, and tap waters were collected at the same place as for the total atmospheric deposition samples. The water samples were collected twice per year from each location in May (wet season) and October (dry season), respectively.

As the most popular food for Haiyan residents, mullet, salsola, rice and crucian carp were collected annually in this work for radioactivity monitoring. Mullet and salsola were locally produced in Haiyan, whereas rice and crucian carp were collected in the Haining City (the primary supplier of rice and crucian carp to local Haiyan population).

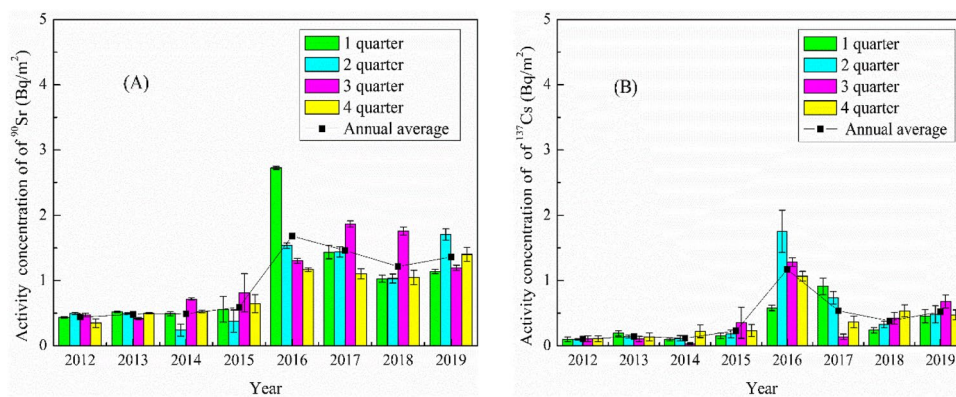


Figure 2. Variation of ⁹⁰Sr (A) and ¹³⁷Cs (B) activity concentration in total atmospheric deposition collected around of QNPP during 2012–2019.

Reagents and standards. Anhydrous alcohol, sulfuric acid, acetone, hydrochloric acid, hydrogen peroxide, nitric acid, oxalic acid, ammonia, and di (2-ethylhexyl) phosphoric acid used for this study were all analytically grade. A ⁹⁰Sr-⁹⁰Y standard solution (9.78 Bq/g of ⁹⁰Sr in 0.1 mol/L nitric acid) and a ¹³⁷Cs standard solution (1.47 Bq/g of ¹³⁷Cs in 0.1 mol/L nitric acid) were purchased from National Institute of Metrology, China. Electroplating source of ⁹⁰Sr-⁹⁰Y with radioactivity intensity (Number of particles on the surface/2π·min) of 1.20 × 10³ was used for calibrating the detection efficiency of the instrument.

Sample preparation and measurement. All dried food samples were placed in a 10 L quartz crucible and ashed with a microwave-ashing furnace (MKX-R4HB, Qingdao Maikewei Microwave Technology Co. Ltd) according to the rapid pretreatment method¹¹ with gradual temperature increase from 100–150 °C to 500 °C (Table S1 in supporting information). All total atmospheric deposition samples were dried on a graphite heating plate (YKM-400C; Changsha Yonglekang Instrument Equipment Co., Ltd.) at 100 °C and then ashed in a muffle furnace (Thermo Fisher Scientific Co., Ltd.) at 450 °C for 8 h.

The radiochemical analysis of ⁹⁰Sr in water and ash samples was according to the Chinese national standard procedures^{12–15}. In general, Sr (100 mg) and Y (20 mg) carriers were added to water (adjusted to pH = 1.0 with concentrated HNO₃) and ash samples. For water samples (50 L of each), SrCO₃/CaCO₃ precipitation was used to pre-concentrate Sr. The SrCO₃/CaCO₃ precipitate was dissolved with 6 mol/L HNO₃ and the sample was adjusted to pH = 1 for further chromatographic purification.

For ash samples (5–30 g), after treated with 3–10 mL of concentrated HNO₃ and 3 mL of H₂O₂, and evaporated to dryness, a second ashing was performed at 600 °C to ensure the complete decomposition of organic substances. Each ash sample was digested with 30–83 mL of 6 mol/L HCl for two times, the combined leachate was proceeded with CaC₂O₄/SrC₂O₄ precipitation for Sr pre-concentration. The CaC₂O₄/SrC₂O₄ precipitate was ashed in a muffle furnace (600 °C, 1 h), and dissolved in 1.5 mol/L HNO₃ for further chromatographic purification.

The processed sample solution for water or ash was loaded onto a chromatographic column (1 cm diameter × 15 cm length) containing di-(2-ethylhexyl) phosphoric acid (HDEHP), at a flow rate of 2 ml/min to separate ⁹⁰Y. The column was washed with 40 mL of 1.5 mol/L HNO₃ at 2 ml/min, and Y was eluted with 30 mL of 6 mol/L HNO₃ at 1 ml/min. The separation time was recorded to calibrate the decay of ⁹⁰Y. Yttrium was finally prepared as oxalate precipitation for gravimetric measurement of Y chemical yields prior to detection with a low background α/β counter (LB790; German Berthold Technology Company). Each sample was counted for 10 cycles, with each cycle for 100 min^{12–15}.

The determination of ¹³⁷Cs in water and ash samples was according to Chinese national standards^{16–19}. Prior to ¹³⁷Cs determination, the samples were kept for one month to allow for a complete decay of ¹³¹I. Each dried food sample was screened with gamma spectrometry to eliminate the interferences of other short-lived radionuclides (¹³⁴Cs, ¹³⁶Cs, and ¹³⁸Cs) on ¹³⁷Cs measurement by beta counting. Cesium carrier (20 mg) was added to the water (50 L, adjusted with nitric acid to pH = 2.0) and ash samples (5–20 g). Cesium contained in each ash sample was leached with 1.5 mol/L HNO₃ for several times. Ammonium phosphomolybdate (AMP) was added to water or leachate sample (from the ash sample) to adsorb cesium. The precipitate was filtered and dissolved in NaOH solution. Cesium was finally separated as Cs₃Bi₂I₉ precipitate in citric acid and acetic acid medium for gravimetric determination of chemical yield and measurement of ¹³⁷Cs using the low background α/β counter. The measurement time was kept 100 min per cycle, in total of 10 cycles for each sample^{16–19}. All the analytical results obtained in this work were summarized in Tables S2, S3, S4 in the supporting information.

Results and discussion

⁹⁰Sr and ¹³⁷Cs activity concentrations in total atmospheric deposition. The ⁹⁰Sr and ¹³⁷Cs activity concentrations in total atmospheric deposition are widely used indicators for revealing potential radioactive pollution in the atmosphere. The inter-annual and seasonal variations in activity concentrations of ⁹⁰Sr and ¹³⁷Cs in total atmospheric deposition collected around QNPP during the period of 2012–2019 are presented in Fig. 2. The observed annual average activity concentrations range within 0.44–1.68 Bq/m² (mean ± sd = 0.97 ± 0.51 Bq/

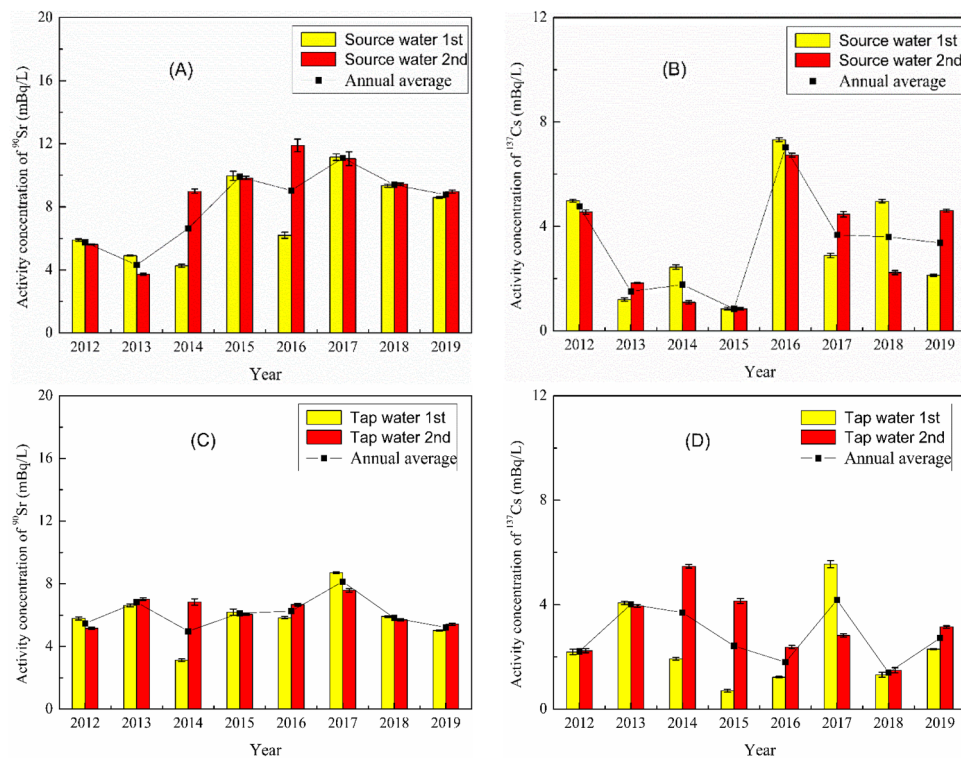


Figure 3. Variation of ^{90}Sr and ^{137}Cs activity concentration in source and tap water collected around QNPP during wet (1st) and dry (2nd) seasons in 2012–2019.

m^2) for ^{90}Sr and $0.10\text{--}1.17\text{ Bq/m}^2$ (mean \pm sd = $0.40 \pm 0.36\text{ Bq/m}^2$) for ^{137}Cs , respectively. ^{90}Sr and ^{137}Cs activity concentrations demonstrate similar inter-annual variabilities across the entire study period, with the lowest annual average constantly obtained in 2012–2015 and the highest values in 2016 followed by a gradual decreasing trend until 2019. The appearance of peak ^{90}Sr and ^{137}Cs activity concentrations in 2016, which are up to ca. 4 and 11 times higher compared to the other years, respectively, potentially indicates additional radioactive plume in the study region in 2016 (see discussion later).

No clear seasonal variations of ^{90}Sr and ^{137}Cs in total atmospheric deposition were observed in this study. Though the highest activity concentrations of ^{90}Sr and ^{137}Cs both occurred in 2016, ^{90}Sr peaked in the first quarter of 2016 whereas ^{137}Cs peaked in the second quarter of 2016. This might be associated to the different source input functions and transport processes between ^{137}Cs and ^{90}Sr . ^{137}Cs is particle reactive and readily attached to aerosols and dust, whereas ^{90}Sr is more water soluble and easier to be dissolved in rainwater²⁰. The late occurrence of ^{137}Cs peak compared to ^{90}Sr peak in 2016 could be due to the association of ^{137}Cs to fine particles suspended in the atmosphere which prolonged the residence time of ^{137}Cs in the atmosphere; and the plum rain in the second quarter (mostly in May) of 2016 flushed the fine particles and thereby prompted the deposition of ^{137}Cs onto the ground. Nevertheless, both ^{90}Sr and ^{137}Cs activity concentrations in the atmosphere around QNPP were generally low in the past decade, and can be considered as baseline concentrations. This low background presents an opportunity to observe any future changes in the ^{90}Sr and ^{137}Cs concentrations and therefore can serve as baseline data for any future inputs from QNPP and other potential nuclear activities.

^{90}Sr and ^{137}Cs activity concentrations in water samples. The time-series of activity concentrations of ^{90}Sr and ^{137}Cs in water samples collected around QNPP during the period of 2002–2019 are plotted in Fig. 3. Except for a few cases, no significant differences are observed for ^{90}Sr and ^{137}Cs activity concentrations in the two type waters between May and October in each year. ^{90}Sr and ^{137}Cs annual average activity concentrations in tap water ($5.0\text{--}8.2\text{ mBq/L}$ for ^{90}Sr and $1.4\text{--}4.2\text{ mBq/L}$ for ^{137}Cs) are relatively stable compared to those in source water ($4.3\text{--}11.1\text{ mBq/L}$ for ^{90}Sr and $0.9\text{--}7.0\text{ mBq/L}$ for ^{137}Cs) during 2012–2019. This should be a consequence of the additional water treatment process (e.g., filtration, disinfection) from raw water to tap water.

The highest ^{90}Sr and ^{137}Cs activity concentrations in source water are observed in 2016, with ^{137}Cs in May and ^{90}Sr in October, respectively. Whereas the peak values for both radionuclides in tap water, as observed in May 2017, seem to appear one year later compared to the source water. This again reflects the human intervention in the water treatment and delivery process. It is also noted that the annual average of ^{137}Cs activity concentration in source water decreased rapidly after 2016 to reach similar level as in 2012, while ^{90}Sr activity concentration was decreasing slowly and still nearly two times higher than the level in 2012. All the measured values for ^{90}Sr and ^{137}Cs activity concentrations in water samples around QNPP during 2012–2019 were below the concentration limits recommended by WHO and Chinese national standards^{21,22} and also comparable to the reported values for waters collected around other NPPs in China (Table 2).

Samples		Tianwan NPP ²³ (sampling time: 2015–2016)	Haiyang NPP ²⁴ (sampling time: 2010–2011)	Sanmen NPP ^{25,26} (sampling time: 2012–2019)	Qinshan NPP (this work)	Chinese regulatory limit ^{21,27}	WHO regulatory limit ²²
⁹⁰ Sr (mBq/L)	Source water	–	2.43–6.47	1.6–9.8	4.3–11.1	100	1000
	Tap water	–	1.21–9.00	1.2–8.3	5.0–8.2	100	1000
¹³⁷ Cs (mBq/L)	Source water	–	–	0.2–8.1	0.9–7.0	10	1000
	Tap water	–	–	0.7–5.1	1.4–4.2	10	1000
⁹⁰ Sr (Bq/kg)*	Rice	<0.007	–	0.04–0.08	0.04–0.5	96	–
	Salsola	0.02–0.4	–	0.07–0.4	0.3–1.1	77	–
	Mullet	0.03–0.05	–	0.2–0.7	0.4–1.1	290	–
	Crucian carp	0.002–0.05	–	0.3–1.2	0.6–1.3	290	–
¹³⁷ Cs (Bq/kg)*	Rice	0.004–0.008	–	0.02–0.081	0.03–0.09	260	–
	Salsola	0.14–0.17	–	0.01–0.07	0.02–0.07	210	–
	Mullet	0.01–0.05	–	0.01–0.03	0.04–0.3	800	–
	Crucian carp	0.01–0.02	–	0.01–0.02	0.04–0.6	800	–

Table 2. Activity concentrations of ⁹⁰Sr and ¹³⁷Cs in water and food samples collected around NPPs in various regions of China. – means there was no relevant data. *Results for food samples were given as Bq/kg fresh weight.

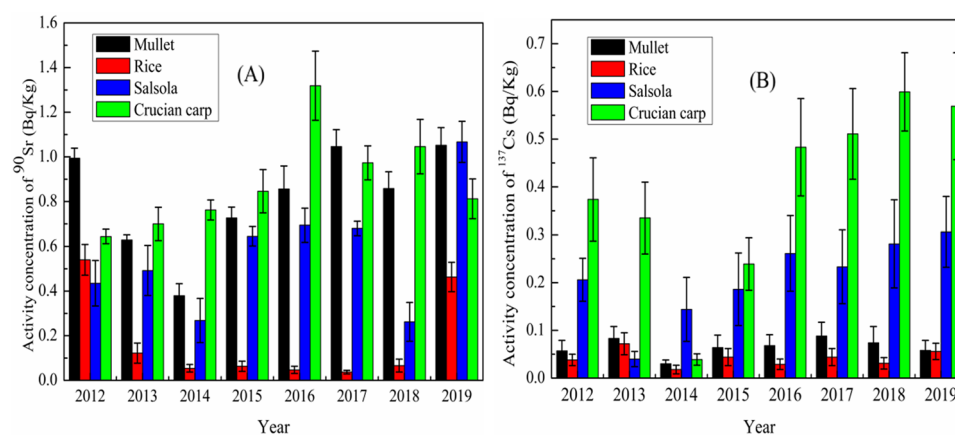


Figure 4. Activity concentrations of ⁹⁰Sr (A) and ¹³⁷Cs (B) in different food samples (mullet, rice, salsola, and crucian carp) collected around QNPP during 2012–2019.

⁹⁰Sr and ¹³⁷Cs activity concentrations in food samples. The activity concentrations of ⁹⁰Sr and ¹³⁷Cs in different types of food samples collected around QNPP during 2012–2019 are presented in Fig. 4. Activity concentrations in rice, salsola, mullet and crucian carp were in the ranges of 0.04–0.5 Bq/kg fresh weight (f. w.), 0.3–1.1 Bq/kg f. w., 0.4–1.1 Bq/kg f. w. and 0.6–1.3 Bq/kg f. w. for ⁹⁰Sr, and 0.03–0.09 Bq/kg f. w., 0.02–0.07 Bq/kg f. w., 0.04–0.3 Bq/kg f. w., and 0.04–0.6 Bq/kg f. w. for ¹³⁷Cs, respectively. Our results are comparable to the activity concentrations of ⁹⁰Sr and ¹³⁷Cs in similar samples collected from other different NPPs in China (Table 2), and far below the Chinese regulatory limit for general foodstuffs.

Though no general trends in the temporal variations of ⁹⁰Sr and ¹³⁷Cs activity concentrations in the four food species can be seen during 2012–2019, the lowest activity concentrations for both radionuclides are mostly observed in rice and the highest values in crucian carp. Interestingly, ⁹⁰Sr activity concentration is often higher in mullet compared to salsola, whereas the opposite is obtained for ¹³⁷Cs. Even between the two fish species, the difference in ¹³⁷Cs activity concentration (up to 10 times) is much higher than that in ⁹⁰Sr activity concentration (max. 1.5 times). These features are linked to ⁹⁰Sr and ¹³⁷Cs levels in the environment where different biota are growing and their different physiological mechanisms for the incorporation and excretion processes of Sr and Cs^{28,29}. For example, mullet inhabits salt water and brackish waters whereas crucian carp is a freshwater fish that inhabits lakes, ponds, and slow-moving rivers.

In the freshwater systems, the high particle/colloid loads may effectively scavenge ¹³⁷Cs, whereas ⁹⁰Sr is kept stable in the water due its highly conservative behavior. Freshwater in some rivers has been found to include high concentrations of ⁹⁰Sr^{30,31}. Besides, higher salinity in brackish water may facilitate the uptake of ¹³⁷Cs (similar to potassium) into the fish. The values of concentration factors for Cs and Sr in marine fishes are 100 and 3, respectively³². Therefore, it is reasonable to expect a larger difference in ¹³⁷Cs activity concentration between mullet and crucian carp compared to that in ⁹⁰Sr activity concentration.

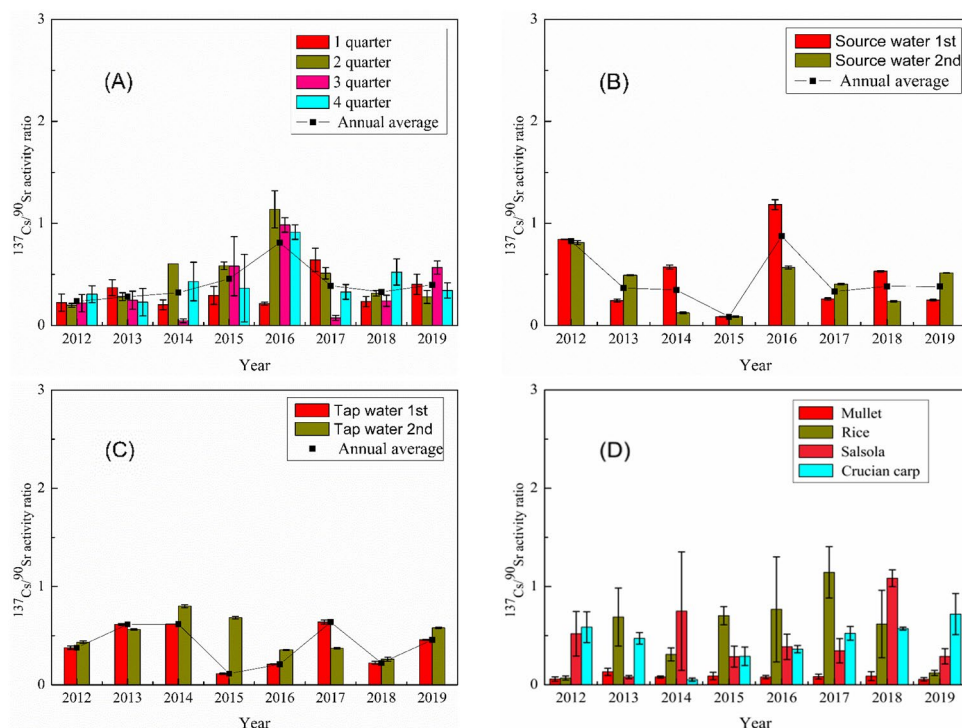


Figure 5. $^{137}\text{Cs}/^{90}\text{Sr}$ activity ratio in total atmospheric deposition (A), source water (B), tap water (C) and food samples (D) during 2012–2019.

The annual effective dose (*AED*) due to the ingestion of ^{137}Cs and ^{90}Sr in foods (i.e., mullet, salsola, rice and crucian carp) were estimated based on the Chinese national standard³³ using the following equation:

$$AED = (I_{\text{Cs}} + I_{\text{Sr}}) \cdot e(g) \quad (1)$$

where I_{Cs} and I_{Sr} is the annual intake of ^{137}Cs and ^{90}Sr in foods (Bq/y), respectively. $e(g)$ was the dose conversion coefficient of ingested radionuclide ^{137}Cs and ^{90}Sr in foods. Dose conversion coefficients of 1.3×10^{-8} Sv/Bq for ^{137}Cs and 2.8×10^{-8} Sv/Bq for ^{90}Sr were used in this study according to the Chinese national standards.

The obtained *AED* through ingestion of ^{137}Cs and ^{90}Sr in foods for the local population around QNPP was calculated to be in the range of 1.3×10^{-4} – 1.1×10^{-3} Sv/y during 2012–2019, with a mean value of $(3.9 \pm 4.0) \times 10^{-4}$ Sv/y. In this calculation, the annual per capita human food consumption (0.19, 0.085, 67.84 and 0.40 kg/year/person for mullet, salsola, rice and crucian carp, respectively) by the local public were according to the survey in 2019 and assumed to be constant during 2012–2019. The estimated mean *AED* for these eight years is considered negligible in respect to the recommended limit (1 mSv/y) established by International Commission on Radiological Protection (ICRP). This reveals that the foods around QNPP were at a safe level during the period 2012–2019.

Source term identification via $^{137}\text{Cs}/^{90}\text{Sr}$ activity ratio. The temporal variations of $^{137}\text{Cs}/^{90}\text{Sr}$ activity ratios in the investigated samples during 2012–2019 are presented in Fig. 5. For total atmospheric deposition, the annual average $^{137}\text{Cs}/^{90}\text{Sr}$ activity ratios ranged from 0.24 to 0.81, with notable peaks observed in 2016. Narrower distribution ranges of $^{137}\text{Cs}/^{90}\text{Sr}$ activity ratios were observed in the water and food samples compared to the total atmospheric deposition, varying within 0.085–1.18 for source water, 0.11–0.80 for tap water, 0.055–0.13 for mullet, 0.069–1.14 for rice, 0.078–1.08 for salsola, 0.052–0.72 for crucian carp, respectively.

The background ^{137}Cs and ^{90}Sr levels on the world surface are mostly due to global fallout of atmospheric nuclear weapons testing during 1945–1980. The activity ratio of $^{137}\text{Cs}/^{90}\text{Sr}$ from the global fallout deposition was estimated to be about 1.6^{34,35}. Our results indicate that all the $^{137}\text{Cs}/^{90}\text{Sr}$ activity ratios are lower than the global fallout signal. This might be associated to faster removal of ^{137}Cs compared to ^{90}Sr originated from global fallout and/or additional input of ^{90}Sr in the surrounding environment of the study region. The latter is very unlikely, because ^{90}Sr concentrations measured in this work are in the background level and there is no record of significant radioactive releases in the study region. Besides, as any potential release of ^{90}Sr (such as civil nuclear industry) would normally be accompanied by ^{137}Cs release and often with much higher $^{137}\text{Cs}/^{90}\text{Sr}$ activity ratios compared to global fallout, owing to the lower volatility of Sr than Cs³⁶. For example, very high $^{137}\text{Cs}/^{90}\text{Sr}$ ratios have been reported in the atmospheric fallout from Fukushima accident (~ 1000)³⁷ and Chernobyl accident (~ 250)³⁸. In seawater, $^{137}\text{Cs}/^{90}\text{Sr}$ ratios reached 39 ± 1 beyond the coast of Japan due to massive liquid releases of

cooling water in spring 2011³⁷. The $^{137}\text{Cs}/^{90}\text{Sr}$ activity ratios before the Fukushima accident were reported in the range of 2.6–18 in Japanese fish whereas the $^{137}\text{Cs}/^{90}\text{Sr}$ activity ratios ranged from 98 to 480 after the accident³⁹.

As ^{137}Cs is more readily adsorbed and immobilized on clay minerals while ^{90}Sr exhibits a higher mobility, it is reasonable to foresee a decrease in global fallout derived $^{137}\text{Cs}/^{90}\text{Sr}$ activity ratios in some freshwater and food samples. This has been approved in earlier studies where activity ratios of $^{137}\text{Cs}/^{90}\text{Sr}$ in wheat and polished rice from Japan increased by nearly 20 and 3 times, respectively, from 1959 to 1995⁴⁰.

^{137}Cs and ^{90}Sr in the dry atmospheric deposition was reported to reflect their signature in the ground-level air, which is mostly from resuspension of the deposited ^{137}Cs and ^{90}Sr in soil⁴¹. Sr is chemically easier to elute than Cs in the soil column by rainwater²⁰, therefore $^{137}\text{Cs}/^{90}\text{Sr}$ activity ratio in the typical surface soil usually becomes higher than the typical global fallout value^{30,31}. However, lower $^{137}\text{Cs}/^{90}\text{Sr}$ activity ratios compared to the global fallout level were observed in the total atmospheric deposition in this work. This might be related to the relative high annual precipitation rate in the study region, therefore the total atmospheric deposition signal are predominated by wet precipitation associated to lower $^{137}\text{Cs}/^{90}\text{Sr}$ activity ratios than global fallout, but are comparable to those measured in fresh waters in this work.

The peak $^{137}\text{Cs}/^{90}\text{Sr}$ activity ratio (1.14 ± 0.18) in the total atmospheric deposition in the second quarter of 2016 was ca. 2.5 times higher than the average values (0.46 ± 0.15) in 2015. This might suggest an additional radioactive input with higher $^{137}\text{Cs}/^{90}\text{Sr}$ activity ratio in the study region in 2016. As a potential consequence of this additional radioactive source, maximum $^{137}\text{Cs}/^{90}\text{Sr}$ activity ratios were observed in the source water (1.18 ± 0.05) in 2016, rice (1.14 ± 0.26) in 2017 and salsola (1.08 ± 0.09) in 2018, respectively. The occurrence of peak $^{137}\text{Cs}/^{90}\text{Sr}$ activity ratio following the sequence of atmosphere-water-biota pinpoints the additional radioactive source might be a direct atmospheric fallout either from local nuclear facilities (e.g., QNPP and other local NPPs) or global sources (e.g., Fukushima accident and others).

It is virtually impossible that the Fukushima fallout arrived to the study region in 2016, five years after the accident. At the first several days of the accidents, air transport in the mid-latitudes was dominated by prevailing westerly winds, which could circle around the globe in 2 weeks⁴². For example, several pulses of radioactive emission from Fukushima were observed in Northern Taiwan 14 days after the accident⁴³. We suspect the potential additional radioactive input in 2016 is from a local source. It was reported that the two units in Fangjiashan NPP (FJSNPP) as an expansion of Phase I in QNPP, were put into operation in December 2014 and February 2015, respectively¹⁰. The commencement of the two units could potentially introduce increased release of ^{137}Cs and ^{90}Sr to some extent. However, this does not support the decrease of ^{137}Cs and ^{90}Sr concentrations and $^{137}\text{Cs}/^{90}\text{Sr}$ activity ratios in the total deposition for the following years. Therefore, further confirmation is needed due lack of operational and discharges data from QNPP in this work.

Conclusions

This study presents the first long-term systematic study of levels, variations and sources of ^{90}Sr and ^{137}Cs in environmental and food samples around QNPP in 2012–2019. The concentrations of ^{90}Sr and ^{137}Cs obtained in this work represent the background level, with all the values below the recommendations by WHO and Chinese national standard. Moreover, the peak concentrations of ^{90}Sr and ^{137}Cs appeared in 2016 were suspected to be related with an additional input from the local facility, but it requires further confirmation. This study indicate the high sensitivity of ^{90}Sr and ^{137}Cs , especially the $^{137}\text{Cs}/^{90}\text{Sr}$ activity ratio for detecting any radioactive release in the region. In the future, ^{90}Sr and ^{137}Cs monitoring is recommended as regional safeguard measure against accidental release from the local nuclear power plant.

Received: 16 August 2021; Accepted: 5 October 2021

Published online: 22 October 2021

References

- IAEA. Nuclear power reactors in the world. Reference data series No. 2. IAEA-RDS-2/36, Vienna, Austria, May 2016: 25±31 (2016).
- Wai, K. M. *et al.* External cesium-137 doses to humans from soil influenced by the Fukushima and Chernobyl nuclear power plants accidents: A comparative study. *Sci. Rep.* **10**, 3575–3590 (2020).
- Canbazoglu, C. & Dogru, M. A preliminary study on ^{226}Ra , ^{232}Th , ^{40}K and ^{137}Cs activity concentrations in vegetables and fruits frequently consumed by inhabitants of Elazig Region, Turkey. *J. Radioanal. Nucl. Chem.* **295**, 1245–1249 (2013).
- Yang, G., Tazoe, H. & Yamada, M. ^{137}Cs activity and $^{137}\text{Cs}/^{137}\text{Cs}$ atom ratio in environmental samples before and after the Fukushima Daiichi nuclear power plant accident. *Sci. Rep.* **6**, 24119 (2016).
- Falandysz, J., Zhang, J. & Zalewska, T. Radioactive artificial ^{137}Cs and natural ^{40}K activity in 21 edible mushrooms of the genus *Boletus* species from SW China. *Environ. Sci. Pollut. Res. Int.* **24**, 8189–8199 (2017).
- Falandysz, J. *et al.* Artificial ^{137}Cs and natural ^{40}K in mushrooms from the subalpine region of the Minya Konka summit and Yunnan Province in China. *Environ. Sci. Pollut. Res. Int.* **25**, 615–627 (2018).
- Salminen-Paatero, S., Thölix, L., Kivi, R. & Paatero, J. Nuclear contamination sources in surface air of Finnish Lapland in 1965–2011 studied by means of ^{137}Cs , ^{90}Sr , and gross beta activity. *Environ. Sci. Pollut. Res. Int.* **26**, 21511–21523 (2019).
- Tazoe, H. *et al.* Observation of dispersion in the Japanese coastal area of released ^{90}Sr , ^{134}Cs , and ^{137}Cs from the Fukushima Daiichi nuclear power plant to the Sea in 2013. *Int. J. Environ. Res. Public Health.* **16**, 4094 (2019).
- Wang, Z. T., Xiang, Y. Y. & Guo, Q. J. Terrestrial distribution of ^{14}C in the vicinity of Qinshan nuclear power plant. *China Radiocarbon* **55**, 59–66 (2013).
- Guo, F., Wu, W. F., Feng, Y. & Shen, H. F. Distribution of tritium concentration in the 0–25 cm surface soil of cultivated and uncultivated soil around the Qinshan nuclear power plant in China. *Appl. Radiat. Isot.* **164**, 109311 (2020).
- Cao, Y. Y. *et al.* Study on rapid microwave-ashing pretreatment method for radioactivity monitoring in food. *Chin. J. Radiol. Med. Prot.* **38**, 43–47 (2018) (in Chinese).
- Environmental Protection Agency of China. Radiochemical analysis of strontium-90 in water Extraction chromatography by di-(2-ethylhexyl) phosphoric acid. Publication No. GB 6766 (1986).

13. Ministry of Environmental Protection of the People's Republic of China. Radiochemical analysis of strontium-90 in water and ash of biological samples. Publication No. HJ 815 (2016).
14. Ministry of Health of the People's Republic of China. Examination of radioactive materials for foods—Determination of strontium-89 and strontium-90. Publication No. GB14883.3 (1994).
15. National Health and Family Planning Commission of the People's Republic of China. National Food Safety Standard—Determination of Radioactive Strontium-89 and strontium-90 in foods. Publication No. GB 14883.3 (2016).
16. Environmental Protection Agency of China. Radiochemical analysis of cesium-137 in water. Publication No. GB 6767 (1986).
17. Ministry of Environmental Protection of the People's Republic of China. Radiochemical analysis of cesium-137 in water and ash of biological samples. Publication No. HJ 816 (2016).
18. Ministry of Health of the People's Republic of China. Examination of radioactive materials for foods—Determination of cesium-137. Publication No. GB 14883.10 (1994).
19. National Health and Family Planning Commission of the People's Republic of China. Examination of radioactive materials for foods - Determination of cesium-137. Publication No. GB 14883.10 (2016).
20. Miller, J. R. & Reitemeier, R. F. The leaching of radiostrontium and radiocesium through soils. *Soil Sci. Soc. Am. J.* **27**, 141–144 (1963).
21. WHO. *Guidelines for Drinking-Water Quality*, 4th ed. (World Health Organization, 2011).
22. General Administration of Quality Supervision, Inspection and Quarantine of the People's Republic of China. Basic standards for protection against ionizing radiation and for the safety of radiation sources. GB 18871-2002 (2003).
23. Lou, H. L. *et al.* Radioactivity levels of ^{137}Cs and ^{90}Sr in organisms and estimation of internal dose around Tianwan nuclear power station. *Nucl. Electron. Detect. Technol.* **38**, 241–244 (2018) (in Chinese).
24. Yang, X., Chen, Y. M., Xu, J. A. & Zhang, L. Investigation and analysis of strontium concentration of drinking-water surrounding Haiyang nuclear power plant. *Chin. J. Radiol. Health* **23**, 193–197 (2014) (in Chinese).
25. Cao, Y. Y. *et al.* Investigation on levels of ^{90}Sr and ^{137}Cs in drinking water and food after installation of the first AP 1000 nuclear power unit in China. *Chin. J. Radiol. Med. Prot.* **41**, 456–460 (2021) (in Chinese).
26. Cao, Y. Y. *et al.* Investigation on levels of gross radioactivity in drinking water and ^{90}Sr in food before and after operation of Sanmen nuclear power plant. *Chin. J. Radiol. Med. Prot.* **40**, 466–471 (2020) (in Chinese).
27. Ministry of Health of the People's Republic of China. Limited concentrations of radioactive materials in foods. GB 14882-94 (1994).
28. Whicker, F. W., Nelson, W. C. & Gallegos, A. F. Fallout ^{137}Cs and ^{90}Sr in trout from mountain lakes in Colorado. *Health Phys.* **23**, 519–527 (1972).
29. Young, D. R. & Folsom, T. R. Cesium accumulation in muscle tissue of marine fishes. *Health Phys.* **37**, 703–706 (1979).
30. Igarashi, Y., Aoyama, M., Hirose, K., Miyao, T. & Yabuki, S. Is it possible to use ^{90}Sr and ^{137}Cs as tracers for the Aeolian dust transport? *Water Air Soil Pollut.* **130**, 349–354 (2001).
31. Ikeuchi, Y. Temporal variations of ^{90}Sr and ^{137}Cs concentrations in Japanese coastal surface seawater and sediments from 1974 to 1998. *Deep Sea Res Part II Top. Stud. Oceanogr.* **50**, 2713–2726 (2003).
32. IAEA. Sediment Distribution Coefficients and Concentration Factors for Biota in the Marine Environment. IAEA Rep. IAEA-ECDOC-422: Vienna, Austria: IAEA, 95 p (2004).
33. General Administration of Quality Supervision, Inspection and Quarantine of the People's Republic of China. Basic Standards for Ionizing Radiation Protection and Radiation Source Safety. Publication No. GB18871 (2002).
34. United Nations Scientific Committee on the Effects of Atomic Radiation. Report to the General Assembly. <http://www.uncsear.org/uncsear/en/publications.html> (2000).
35. Krey, P. W. & Krajewsky, B. Comparison of atmospheric transport model calculations with observations of radioactive debris. *J. Geophys. Res.* **75**, 2901–2908 (1970).
36. Nuclear Emergency Response Headquarters, Government of Japan, 2011. Report of the Japanese government to the IAEA ministerial conference on nuclear safety. http://www.kantei.go.jp/foreign/kan/topics/201106/houkokusho_e.html (Accessed 27 Jan 2014)
37. Castrillejo, M. *et al.* Reassessment of ^{90}Sr , ^{137}Cs and ^{134}Cs in the coast off Japan derived from the Fukushima Dai-ichi nuclear accident. *Environ. Sci. Technol.* **50**, 173–180 (2016).
38. Irlweck, K., Khademi, B., Henrich, E. & Kronraff, R. $^{239(240),238}\text{Pu}$, ^{90}Sr , ^{103}Ru and ^{137}Cs concentrations in surface air in Austria due to dispersion of Chernobyl releases over Europe. *J. Environ. Radioact.* **20**, 133–148 (1993).
39. Miki, S. *et al.* Concentrations of ^{90}Sr and $^{137}\text{Cs}/^{90}\text{Sr}$ activity ratios in marine fishes after the Fukushima Dai-ichi nuclear power plant accident. *Fish. Oceanogr.* **26**, 221–233 (2017).
40. Metz, S., Shozugawa, K. & Steinhauser, G. Analysis of Japanese radionuclide monitoring data of food before and after the Fukushima nuclear accident. *Environ. Sci. Technol.* **49**, 2875–2885 (2015).
41. Povinec, P. P. *et al.* Long-term variations of ^{14}C and ^{137}Cs in the Bratislava air: Implications of different atmospheric transport processes. *J. Environ. Radioact.* **108**, 33–40 (2012).
42. Uno, I. *et al.* Asian dust transported one full circuit around the globe. *Nat. Geosci.* **2**, 557–560 (2009).
43. Huh, C. A., Hsu, S. C. & Lin, C. Y. Fukushima-derived fission nuclides monitored around Taiwan: Free tropospheric versus boundary layer transport. *Earth Planet. Sci. Lett.* **319–320**, 9–14 (2012).

Author contributions

Y.C.: study design; collection, analysis, and interpretation of data; and final approval of the manuscript. Z.Z., P.W., S.Y., Z.L., M.Z., X.G., Y.Z., Z.X., H.R., D.Z., X.L.: study design; collection, detection, analysis, and interpretation of data; and manuscript writing.

Funding

This work was supported by Zhejiang Provincial Public Welfare Technology Application Research Project (LGC21H260001), and Zhejiang Health Science and Technology Plan (2021KY613 and 2021KY956), and Open Foundation of Beijing Key Laboratory of Occupational Safety and Health (2021), and Scientific research projects of agriculture and social development in Hangzhou (20201203B220).

Competing interests

The authors declare no competing interests.

Additional information

Supplementary Information The online version contains supplementary material available at <https://doi.org/10.1038/s41598-021-00114-y>.

Correspondence and requests for materials should be addressed to X.L.

Reprints and permissions information is available at www.nature.com/reprints.

Publisher's note Springer Nature remains neutral with regard to jurisdictional claims in published maps and institutional affiliations.



Open Access This article is licensed under a Creative Commons Attribution 4.0 International License, which permits use, sharing, adaptation, distribution and reproduction in any medium or format, as long as you give appropriate credit to the original author(s) and the source, provide a link to the Creative Commons licence, and indicate if changes were made. The images or other third party material in this article are included in the article's Creative Commons licence, unless indicated otherwise in a credit line to the material. If material is not included in the article's Creative Commons licence and your intended use is not permitted by statutory regulation or exceeds the permitted use, you will need to obtain permission directly from the copyright holder. To view a copy of this licence, visit <http://creativecommons.org/licenses/by/4.0/>.

© The Author(s) 2021